

**Polarons in Narrow Band-Gap Polymers Probed over the Entire IR Range: a Joint  
Experimental and Theoretical Investigation**

Simon Kahmann,<sup>1,2</sup> Daniele Fazzi,<sup>3</sup> Gebhard J. Matt,<sup>1</sup> Walter Thiel,<sup>3</sup> Maria A. Loi,<sup>2</sup> Christoph J. Brabec<sup>1,4</sup>

1 Institute for Materials for Electronics and Energy Technology (i-MEET), Friedrich-Alexander University  
Erlangen-Nürnberg, Martensstraße 7 D-91058 Erlangen, Germany.

2 Zernike Institute for Advanced Materials, Rijksuniversiteit Groningen, Nijenborgh 4 Groningen, NL-9747 AG,  
The Netherlands.

3 Max-Planck-Institut für Kohlenforschung (MPI-KOFO), Kaiser-Wilhelm-Platz 1, D-45470 Mülheim an der  
Ruhr, Germany.

4 Bavarian Center for Applied Energy Research (ZAE Bayern), Haberstraße 2a, D-91058, Erlangen, Germany

1. Experimental:

**Measurements**

Thin films were either drop- or spin-cast from solution (CB for C-PCPDTBT and oDCB for Si-PCPDTBT, both at 20 mg/mL) on ZnSe platelets in a glove box. The spinning speed was around 1200 rpm which lead to thicknesses of approximately 150 nm. The samples were then mounted into a cryostat without being exposed to air and positioned in the beam path of the Bruker Vertex 70 FTIR spectrometer. The beam passes two ZnSe windows and is detected using a liquid nitrogen cooled MCT detector. For the MIR we employed a KBr beamsplitter and switched to quartz for the NIR. The sample, being cooled down to 77 K as well, is positioned under 45° to allow

for the pump light being sent through an additional quartz window. To avoid influences by the pump light, we furthermore placed a filter (Ge for the MIR and an appropriate long pass glass filter in the NIR) in front of the detector. Spectra were acquired with a resolution of 5 cm<sup>-1</sup> in the MIR (10 cm<sup>-1</sup> in the NIR) and the following cycle was run at least 512 times: first, the pump is switched on followed by a delay of 1.5 s to establish equilibrium, which is followed by a 16 fold averaging of the "light on" spectrum. Next, the light is switched off followed by another 1.5 s delay and 16 co-additions for the "light off" spectrum. The "light off" spectrum is also used as transmission measurement.

As can be seen from Figure 1 in the main part, the spectra become noisier towards high energies which is mostly related to a reduction in detector sensitivity, but more importantly to a fading light intensity of our probe light. Especially for region where the polymer starts to absorb we are not able to monitor meaningful spectra anymore. We thus do not show the well-known transition to the ground state bleach (GSB) at energies slightly higher than 1.5 eV. Furthermore, since we do not use monochromators in our set-up, but rather rely on the Fourier transformation, edge effects can have an impact on the overall course of the spectra.

## Calculations

DFT and (TD)DFT calculations were performed using the range-separated  $\omega$ B97X-D functional, with inclusion of Grimme's dispersion corrections, with double and triple split Pople basis set with diffusion functions (6-31G\* and 6-311G\*). Restricted and unrestricted DFT calculations were carried out for the neutral ground state ( $S_0$ ), singlet excited states ( $S_1$  and  $S_g$ ), the lowest triplet state ( $T_1$ ) and charged electronic states ( $\pm 1$ ,  $\pm 2$ ), respectively. Geometries were optimized without constraints in each electronic state considered. Equilibrium geometries were characterized by evaluating the Hessian matrix. For charged species ( $\pm 1$ ,  $\pm 2$ ), whenever an instability in the wavefunction was encountered, the geometries were fully relaxed for the lowest UDFT-BS solution. IR vibrational spectra and optical transitions were evaluated for each species at the optimized equilibrium geometry. Intra-molecular properties were evaluated for C- and Si-PCPDTBT oligomers with four and eight repeat units ( $n = 4, 8$ ), with alkyl chains being replaced by methyl groups. Inter-molecular properties were evaluated for model dimers built from  $\pi$ -stacked oligomers. Different dimer models were considered, namely: pairs of two-, three-, and four-unit oligomers. For each aggregate, neutral and charged ( $\pm 1$ ,  $\pm 2$ ) electronic states were considered at the DFT, UDFT, and UDFT-BS levels. Electronic transitions were evaluated at the (TD)DFT and/or (TD)UDFT-BS level.

Details concerning i) the Cartesian coordinates of the optimized geometries, ii) the stabilization energies of the UDFT-BS solutions, and iii) the electronic transitions investigated and their characterizations, are reported below.

## 2. Additional comparisons of the experimental spectra in the MIR:

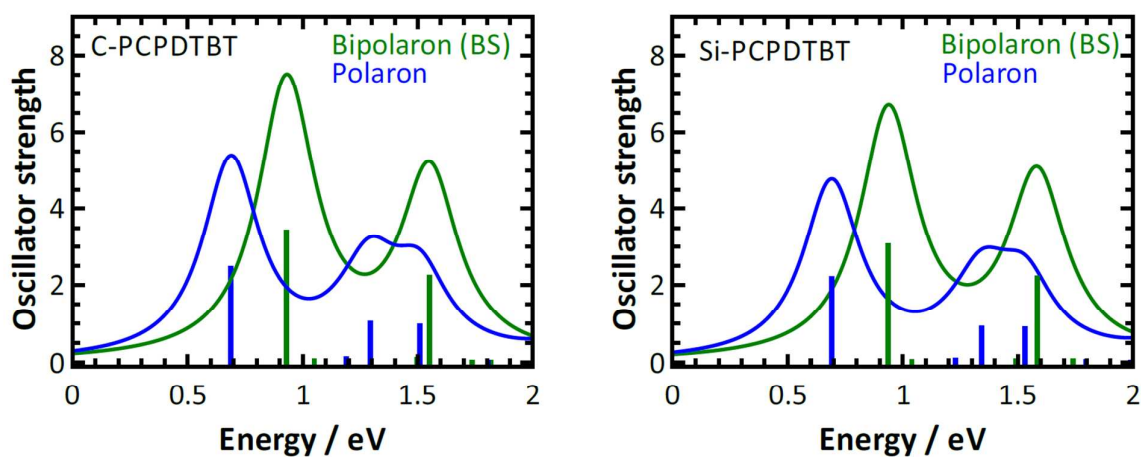


Figure S 1: Simulated transition energies of polarons and bipolarons of C- (left) and Si-PCPDTBT (right) calculated at the TDDFT level ( $\omega$ B97X-D/6-31G\*).

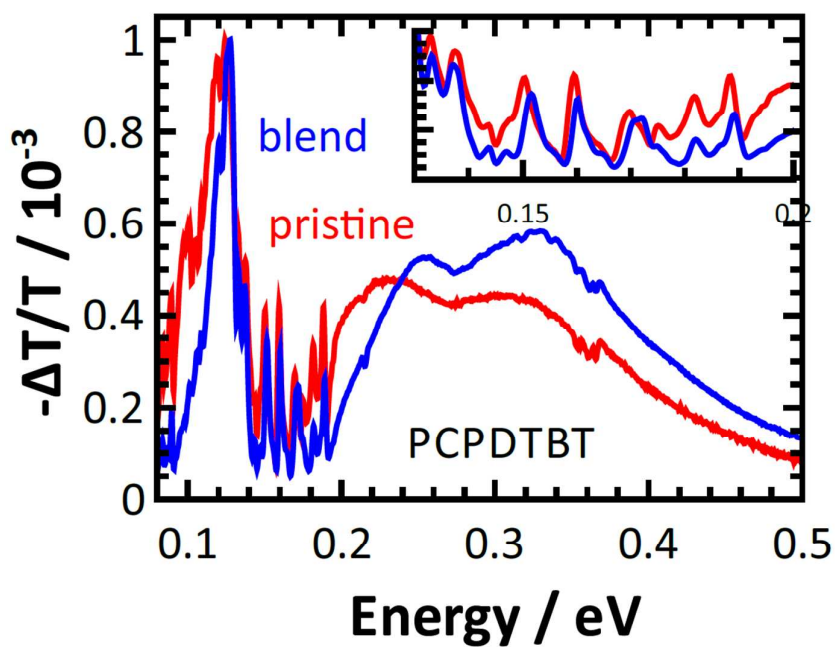


Figure S 2: PIA spectra of pristine PCPDTBT (red) and the blend with PCBM (blue) using an excitation wavelength of 532 nm. The inset depicts a close-up of the IRAV region.

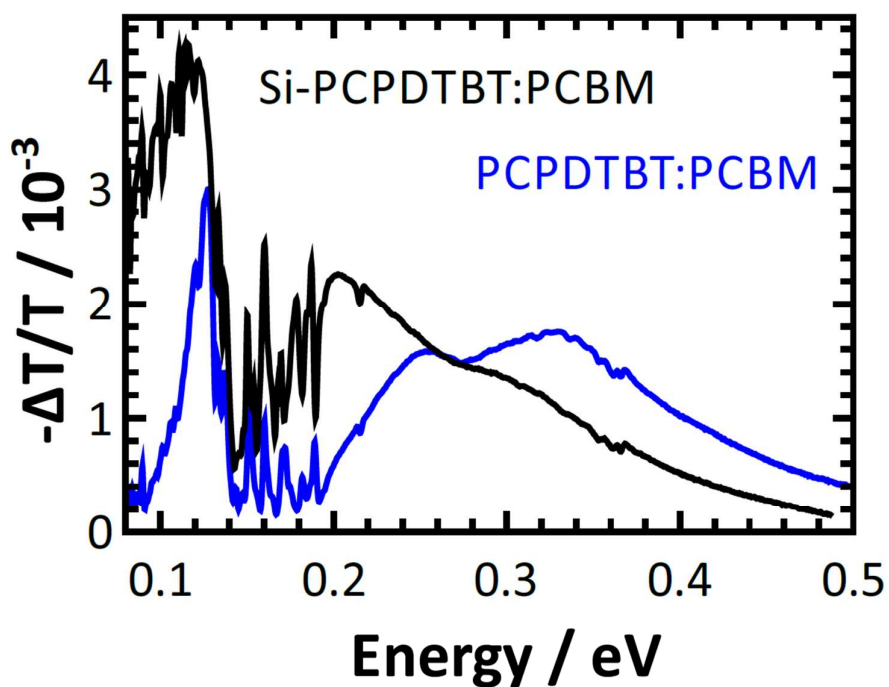


Figure S 3: Comparison of the two employed polymers when blended with PCBM upon excitation with 532 nm. Whereas the IRAV positions are almost identical, the broad electronic features seem red-shifted for Si-PCPDTBT.

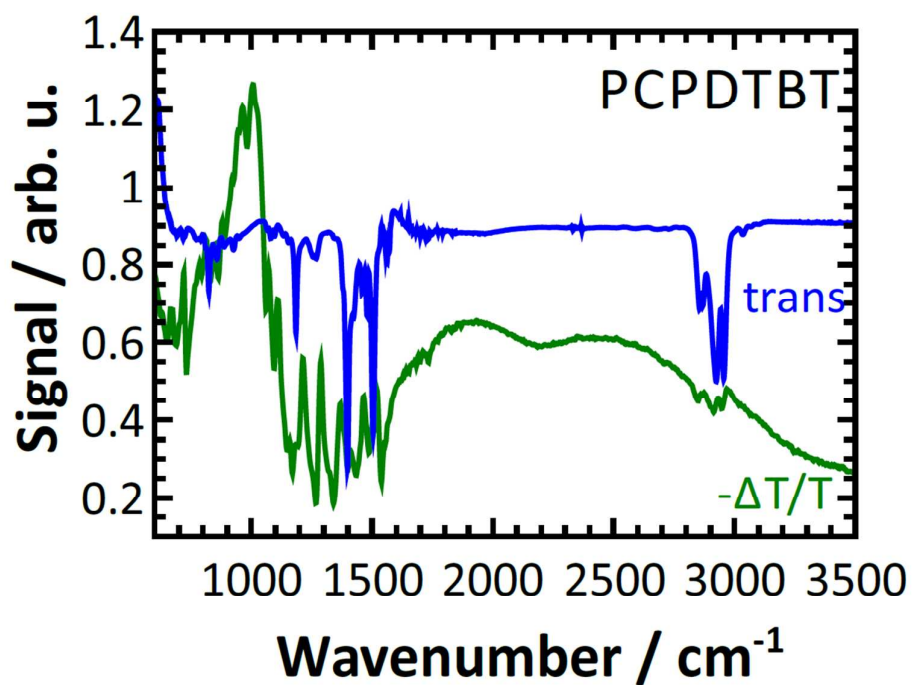


Figure S 4: Comparison between PCPDTBTB PIA spectrum with the transmission in the MIR. As can be seen, strong vibrations in the transmission are no necessity for IRAVs.

### 3. Calculated electronic transition energies for possibly involved species:

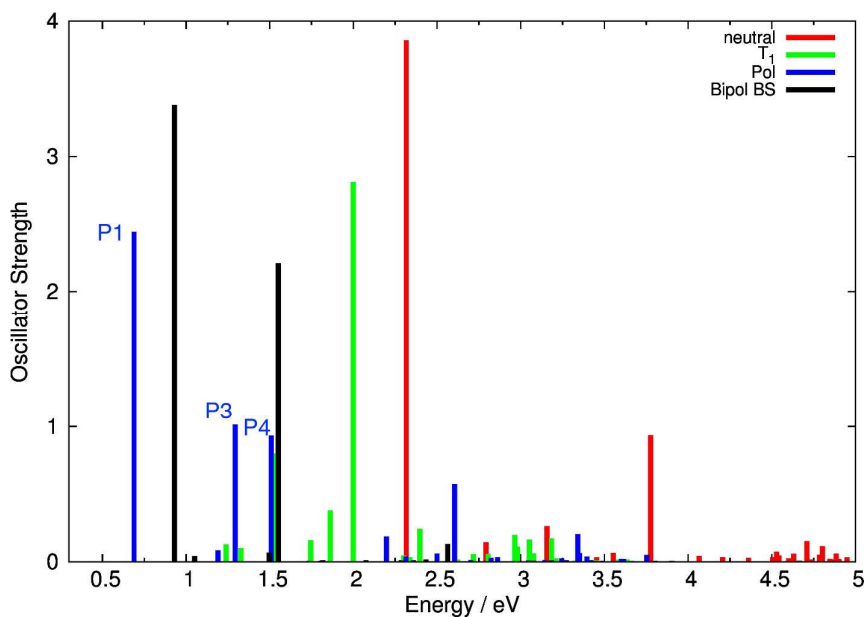


Figure S 5: Electronic vertical transition energies computed at the TDDFT level ( $\omega$ B97X-D/6-31G\*) for PCPDTBT4 oligomer in different electronic states, namely: neutral ground state (red), lowest triplet state (T<sub>1</sub>, green), polaron state (blue), bipolaron state described at the UDFT-BS (black).

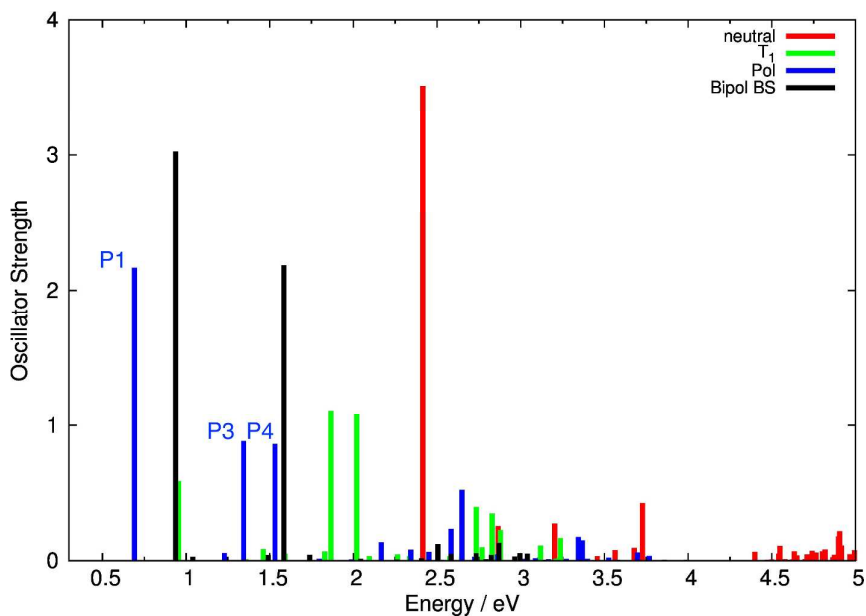


Figure S 6: Electronic vertical transition energies computed at the TDDFT level ( $\omega$ B97X-D/6-31G\*) for Si-PCPDTBT4 oligomer in different electronic states, namely: neutral ground state (red), lowest triplet state (T<sub>1</sub>, green), polaron state (blue), bipolaron state described at the UDFT-BS level (black).

#### 4. Calculated spectra for the negative polarons:

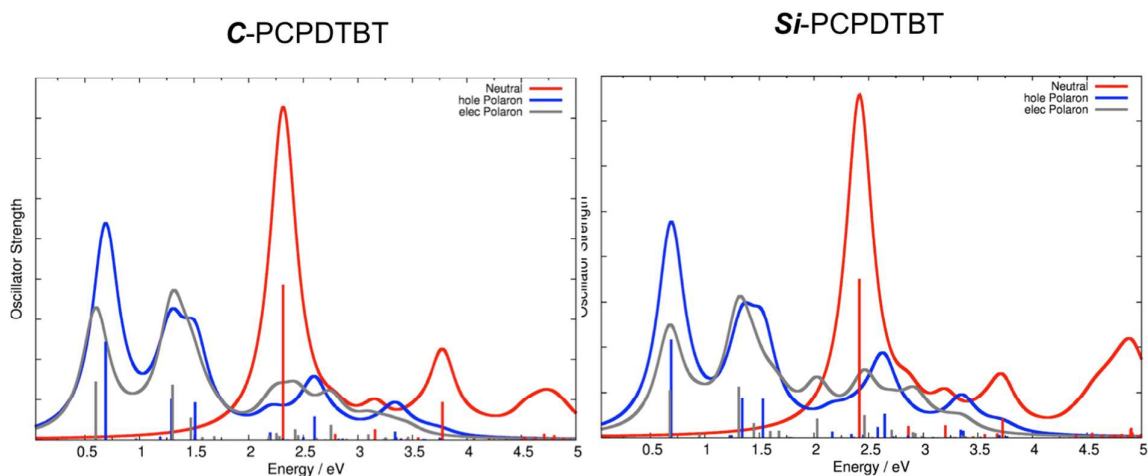


Figure S 7: Electronic vertical transition energies and spectra computed at the TDDFT level ( $\omega$ B97X-D/6-31G\*) for C- (left panel) and Si-PCPDTBT<sub>4</sub> (right panel) oligomer. Neutral (red) state, positive (blue) and negative (gray) polaron states are computed for both polymers.

#### 5. Electron-hole densities and transition energies for different transitions and configurations:

##### Electron-hole density

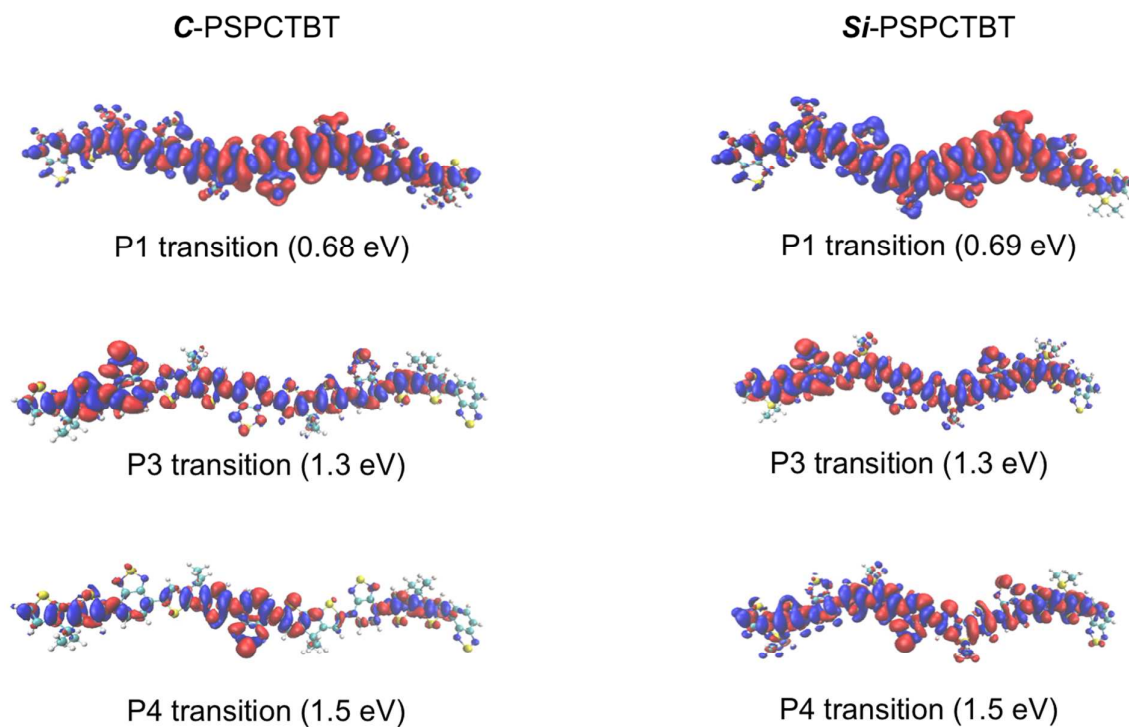
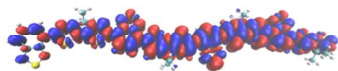


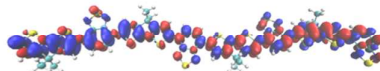
Figure S 8: Electron-hole density maps for the relevant polaronic transitions (herein named P1, P3 and P4, as reported in Figure S6 and S7) for PCPDTBT<sub>4</sub> and Si-PCPDTBT<sub>4</sub>.

## Spin density

### Oligomers ( $n = 4$ )

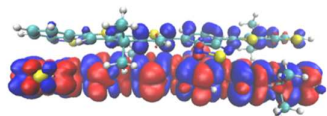


UDFT polaron –  $n = 4$

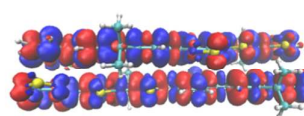


UDFT-BS bipolaron –  $n = 4$

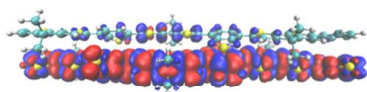
### Aggregates ( $2 \times n$ )



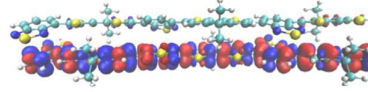
UDFT polaron –  $n = 2$   
dimer



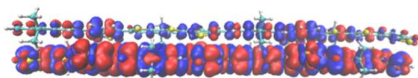
UDFT-BS bipolaron –  $n = 2$   
dimer



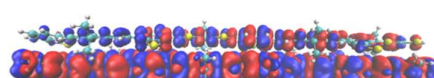
UDFT polaron –  $n = 3$  dimer



UDFT-BS bipolaron –  $n = 3$   
dimer



UDFT polaron –  $n = 4$  dimer



UDFT-BS bipolaron –  $n = 4$   
dimer

Figure S 9: Polaron and bipolaron spin density ( $\uparrow$  and  $\downarrow$  contributions) for PCPDTBT oligomer ( $n = 4$ ) (top) and aggregates (bottom). Aggregates are defined as molecular dimers constituted by oligomers featuring different chain-lengths, namely  $n = 2, 3, 4$ . UDFT or UDFT-BS methods were adopted in the geometry optimization and properly calculation.

Table S 1: Energy difference ( $\Delta E$ ) between the unrestricted DFT – broken symmetry (UDFT-BS) and unrestricted DFT (UDFT) solutions for the case of PCPDTBT<sub>4</sub> and Si-PCPDTBT<sub>4</sub> bipolaron. Values are expressed in eV.

	PCPDTBT	Si-PCPDTBT
$n = 4$	-0.651	-0.721

Table S 2: Low-lying vertical electronic transitions energy and oscillator strengths, computed at the TD-UDFT or TD-UDF-BS level (depending on the most stable solution) for single charged (i.e. polaron)  $2 \times \text{PCPDTBT}_n$  aggregates.

<i>single charged</i>	Aggregate $2 \times n=2$ eV (oscillator strength)	Aggregate $2 \times n=3$ eV	Aggregate $2 \times n=4$ eV
S1	0.9296 (0.73)	0.8468 (1.23)	0.6284 (0.05)
S2	0.9972 (0.02)	0.9967 (0.016)	0.7254 (2.45)
S3	1.2000 (0.004)	1.1182 (0.008)	0.7973 (0.046)



S4	1.4782 (0.33)	1.2582 (0.021)	0.9397 (0.24)
----	------------------	-------------------	------------------

**Table S 3: Low-lying vertical electronic transitions energy and oscillator strengths, computed at the TD-UDFT or TD-UDF-BS level (depending on the most stable solution) for double charged (i.e. two polarons or one bipolaron) 2xPCPDTBT<sub>n</sub> aggregates.**

<i>double charged</i>	Aggregate 2 x n=2 eV (oscillator strength)	Aggregate 2 x n=3 eV	Aggregate 2 x n=4 eV
S1	0.6145 (0.01)	0.8183 (0.03)	0.6518 (0.00002)
S2	1.1267 (0.9)	0.8620 (0.05)	0.8001 (0.1)
S3	1.4622 (0.002)	1.0907 (1.7)	0.8461 (3.26)
S4	1.5037 (0.00002)	1.1411 (0.01)	1.0073 (0.0005)

**Table S 4: Energy difference ( $\Delta E$ ) between the unrestricted DFT – broken symmetry (UDFT-BS) and unrestricted DFT (UDFT) solutions for the case of PCPDTBT monomers (i.e. PCPDTBT4) and dimers featuring different monomer lengths (i.e. 2 x n=2, 2 x n=3, 2 x n=4). Spin contamination values are also reported.**

		$\Delta E \text{ (UDFT-BS – UDFT)} / \text{eV}$ $\langle S^2 \rangle$		
<i>monomer</i>		<i>neutral</i>	<i>polaron</i>	<i>bipolaron</i>
	<i>n = 4</i>	0	0 (0.80)	-0.65 (3.44)
	<i>dimer</i>			
	<i>n = 2</i>	0	0 (0.76)	-0.36 (2.59)
	<i>n = 3</i>	0	-0.10 (0.79)	-0.40 (2.59)
	<i>n = 4</i>	0	0 (0.78)	-0.44 (5.17)

## 6. Comparison of transition upon changing the level of theory:

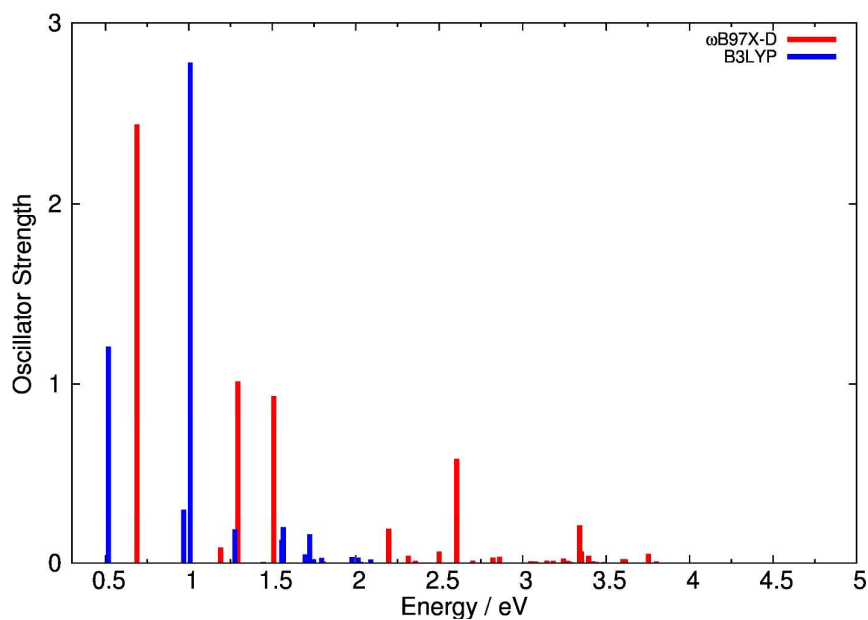
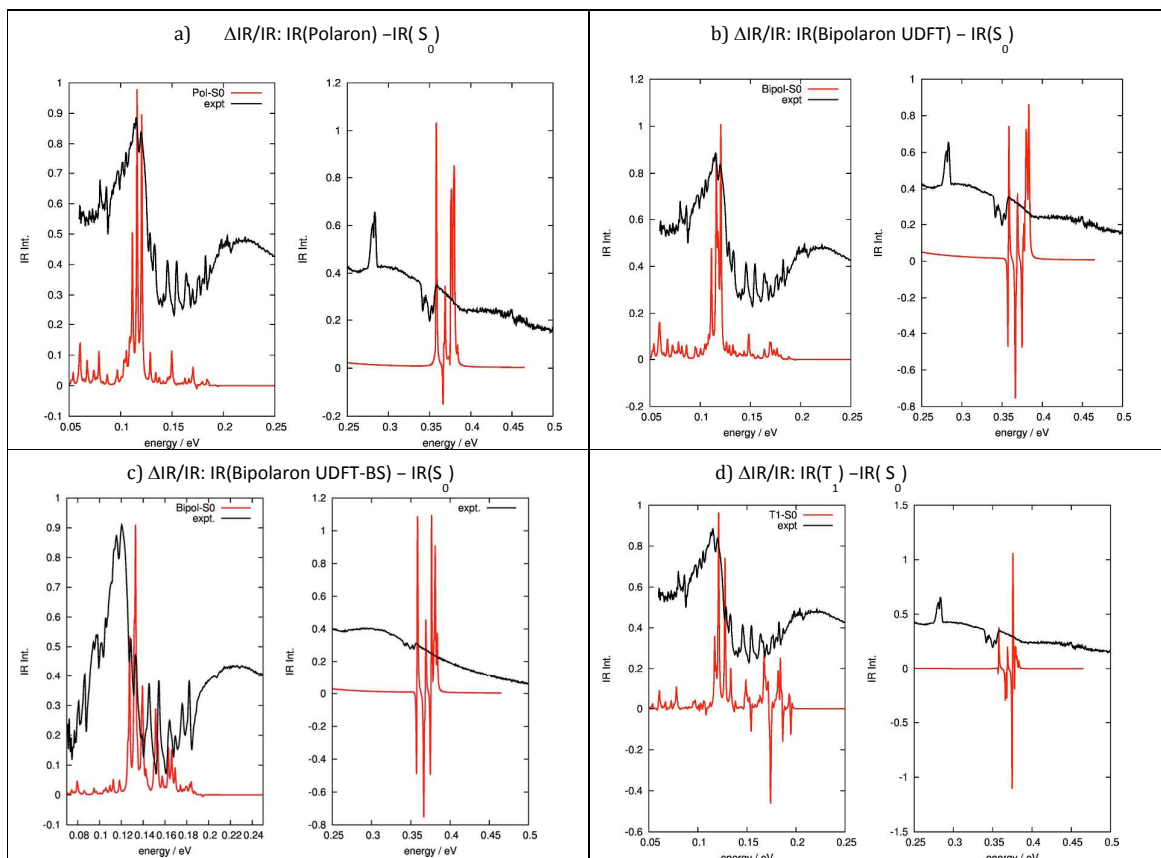
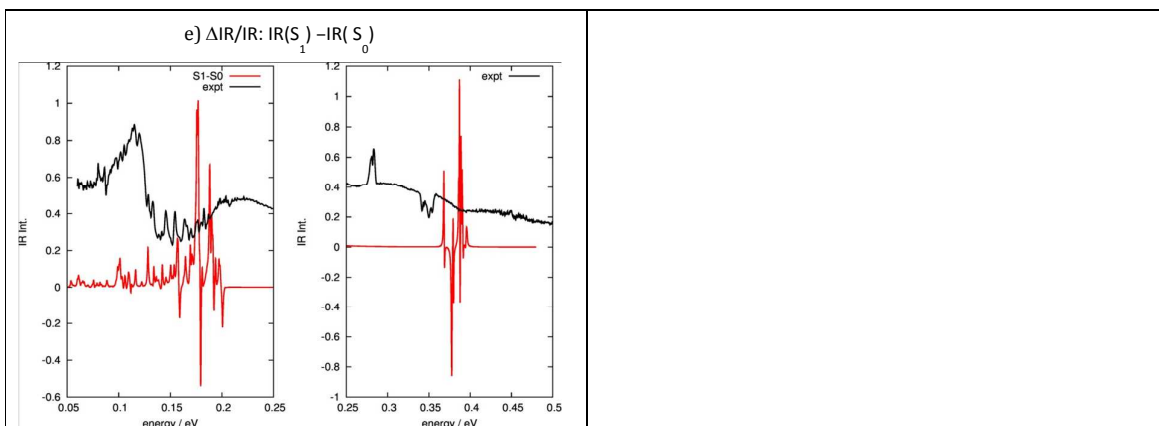


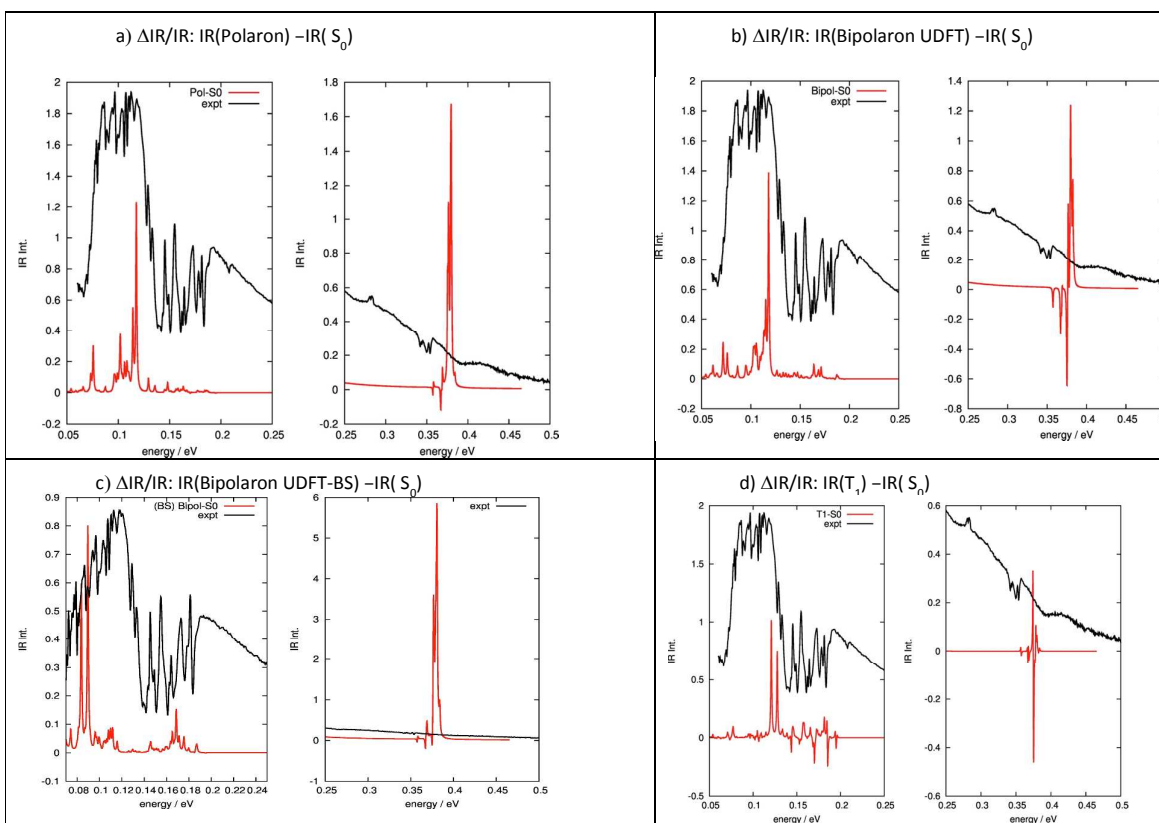
Figure S 10: Comparison between the polaron TD-UDFT vertical transition energies as computed at the  $\omega$ B97X-D (red) and B3LYP (blue) level of theory for PCPDTBT<sub>4</sub>.

#### 7. Calculated PIA spectra in the infrared for different species:





**Figure S 11: Comparison between experimental (black) and computed PIA spectra for PCPDTBT4 in different electronic states. Case a) Polaron species; case b) bipolaron (UDFT) species; case c) bipolaron (UDFT-BS) species; case d) triplet T1 species; case e) singlet excited state  $S_1$ . Theoretical spectra obtained subtracting the IR spectra for the excited state/charged species from the ground state  $S_0$ .**



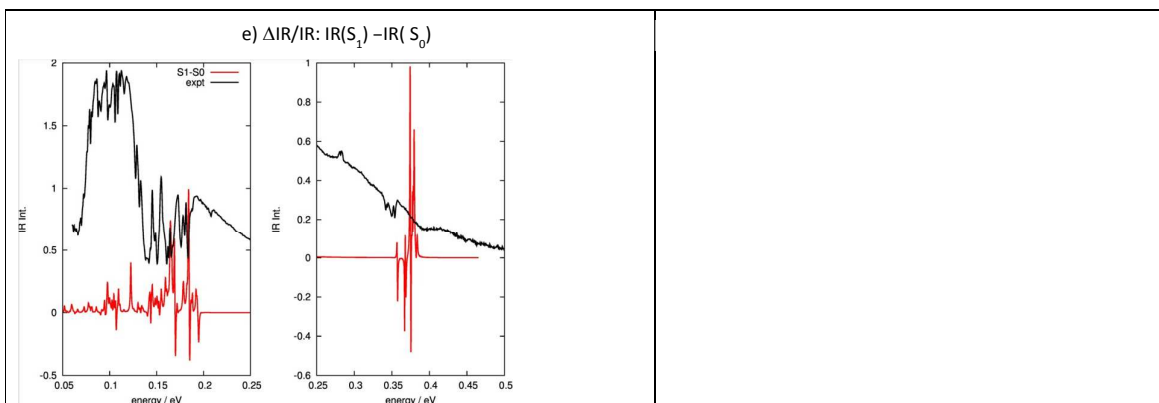


Figure S 12: Comparison between experimental (black) and computed PIA spectra for Si-PCPDTBT4 in different electronic states. Case a) Polaron species; case b) bipolaron (UDFT) species; case c) bipolaron (UDFT-BS) species; case d) triplet T1 species; case e) singlet excited state S1. Theor

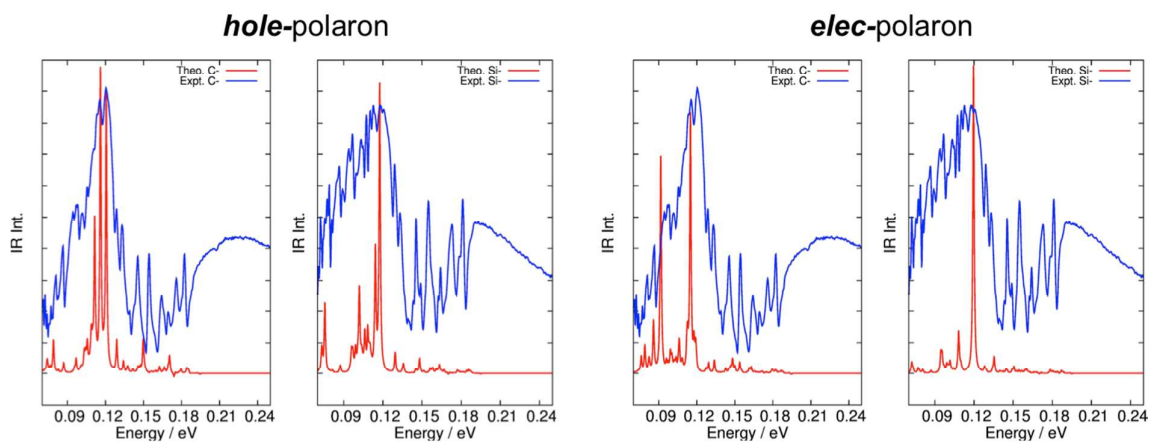


Figure S 13: Comparison between experimental (black) and computed PIA spectra for C- and Si-PCPDTBT<sub>4</sub> in the case of hole (left) and electron (right) polaron.

## 8. Experimental PIA spectra upon varying the excitation wavelength:

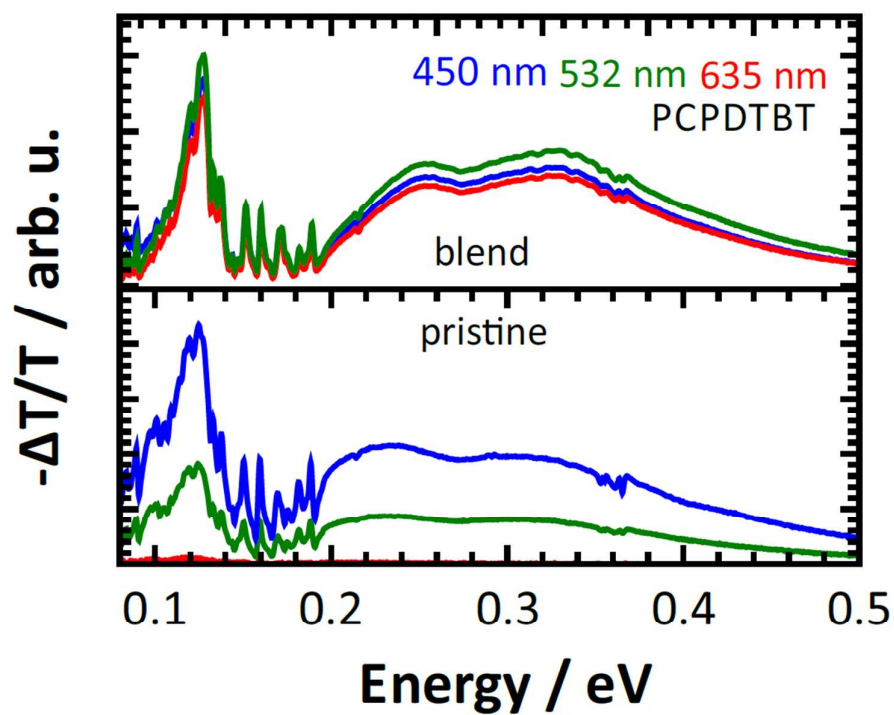


Figure S 14: PIA spectra of a pristine Si-PCPDTBT film and the blend with PCBM upon illumination with 450 (blue), 532 (green) and 635 (red) nm.

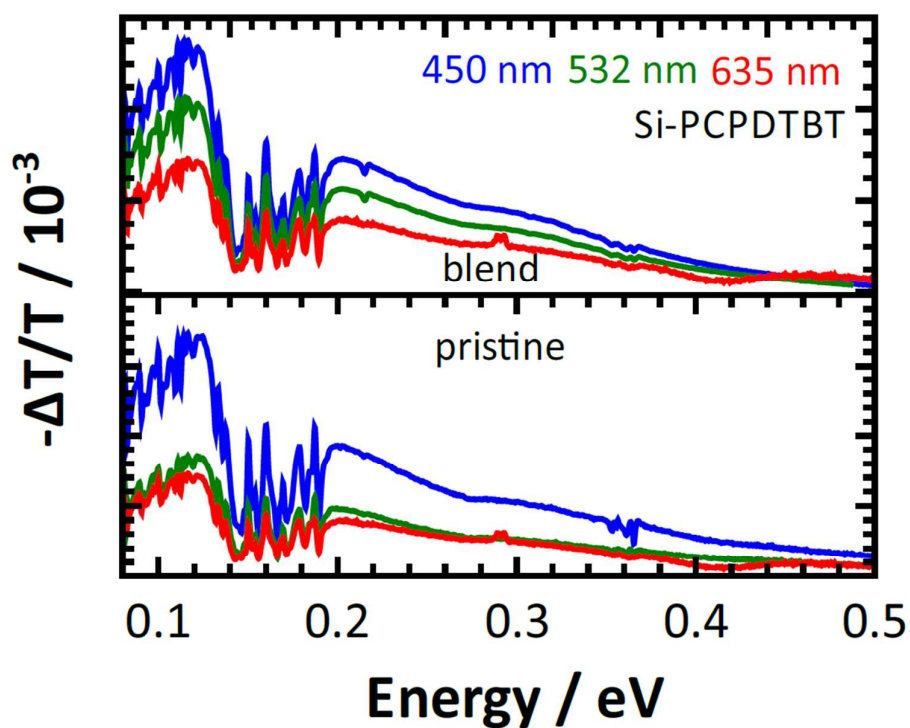


Figure S 15: PIA spectra of a pristine Si-PCPDTBT film and the blend with PCBM upon illumination with 450 (blue), 532 (green) and 635 (red) nm.